Supporting information

Crystallization and Conformation Engineering of Solution-process Polymer Transparent Electrodes with High Conductivity

Aifeng Hu[a], Licheng Tan[a,b], Xiaotian Hu[a], Lin Hu[a], Qingyun Ai[a], Xiangchuan Meng[a], Lie Chen*[a,b] and Yiwang Chen*[a,b]

[a]College of Chemistry, Nanchang University, 999 Xuefu Avenue, Nanchang 330031, China

[b]Jiangxi Provincial Key Laboratory of New Energy Chemistry/Institute of Polymers, Nanchang University, 999 Xuefu Avenue, Nanchang 330031, China

Corresponding author. Tel.: +86 791 83968703; fax: +86 791 83969561. E-mail: ywchen@ncu.edu.cn (Y. Chen), chenlie@ncu.edu.cn (L. Chen).

Author contributions. A. Hu, L. Tan and X. Hu contributed equally to this work.

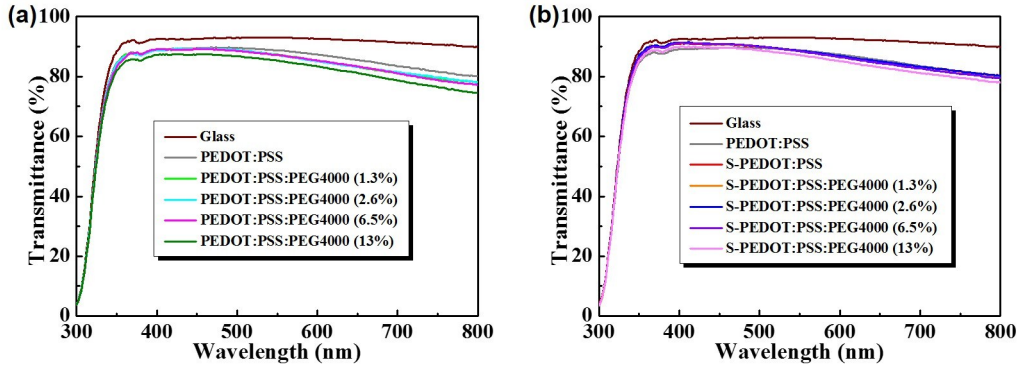

Figure S1. (a) The transmittance spectra of glass, pristine PEDOT:PSS and modified PEDOT:PSS by polyethylene glycol 4000 (PEG4000) with various weight ratios in the range from 300 nm to 800 nm. (b) The transmittance spectra of glass, pristine PEDOT:PSS, H_2SO_4-treated PEDOT:PSS (S-PEDOT:PSS), S-PEDOT:PSS (~40 nm) with various weight ratios of PEG4000 in the range from 300 nm to 800 nm.

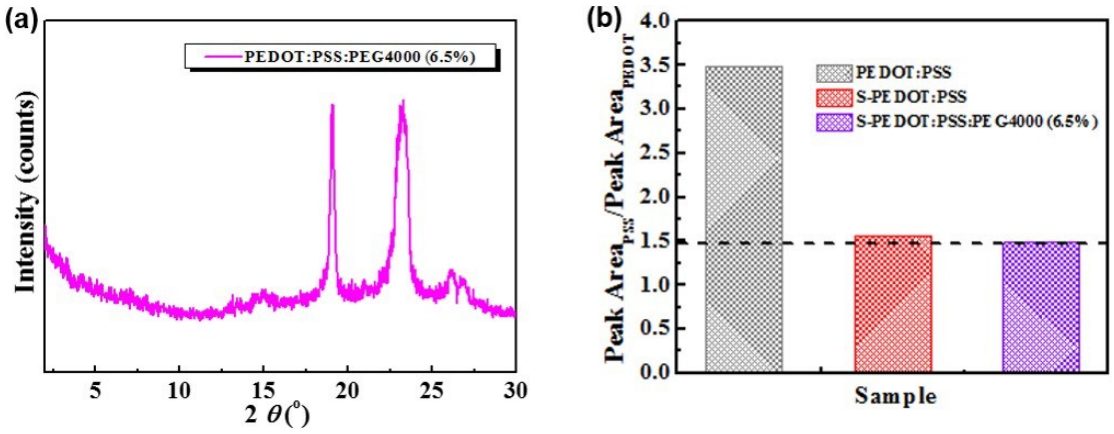

Figure S2. X-ray diffraction (XRD) pattern of PEDOT:PSS with 6.5 wt% PEG4000 (PEDOT:PSS:PEG4000 (6.5%)) in the range from 2° to 30°. (b) The peak area ratios of PSS to PEDOT of pristine PEDOT:PSS, S-PEDOT:PSS and H_2SO_4-treated PEDOT:PSS with 6.5 wt% PEG4000 (S-PEDOT:PSS:PEG4000 (6.5%)) in X-ray photolelectron spectroscopy (XPS) S(2p) spectra by XPS peak processing.

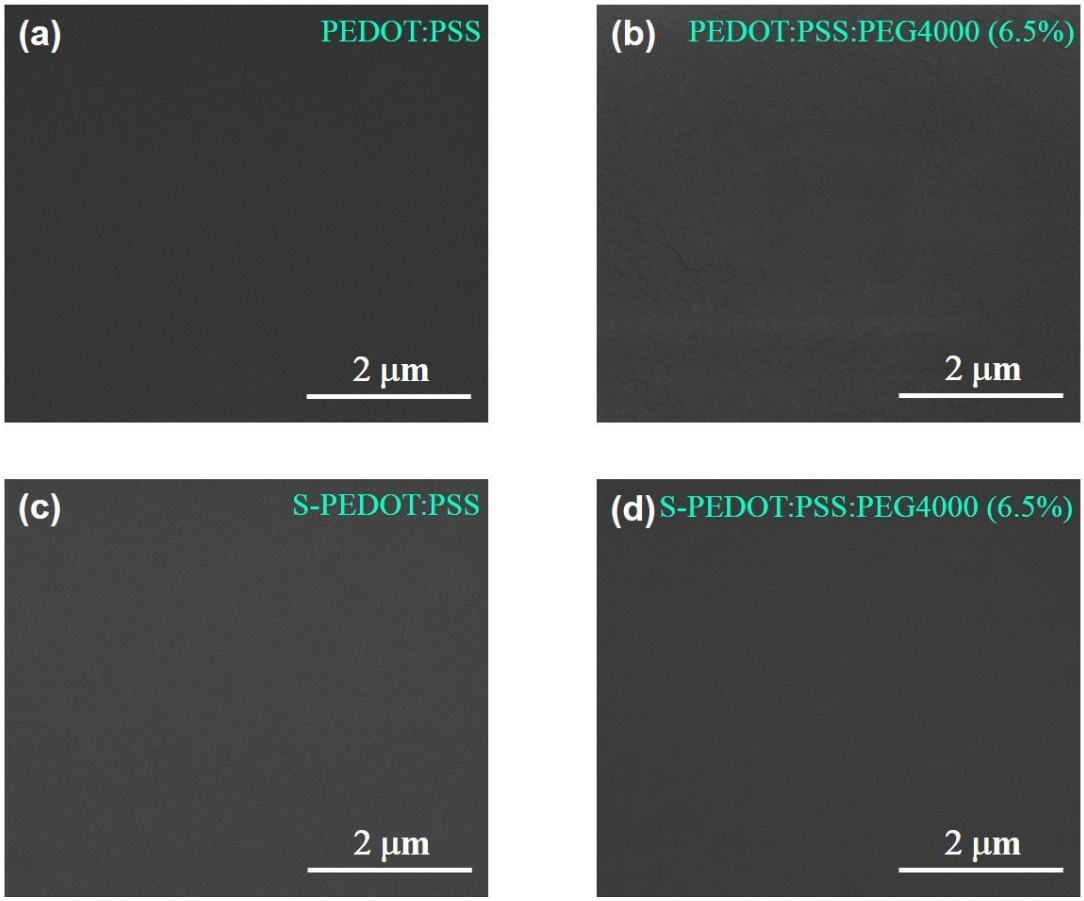

Figure S3. Low-magnification scanning electron microscopy (SEM) images of (a) pristine PEDOT:PSS, (b) PEDOT:PSS:PEG4000 (6.5%), (c) S-PEDOT:PSS and (d) S-PEDOT:PSS:PEG4000 (6.5%).

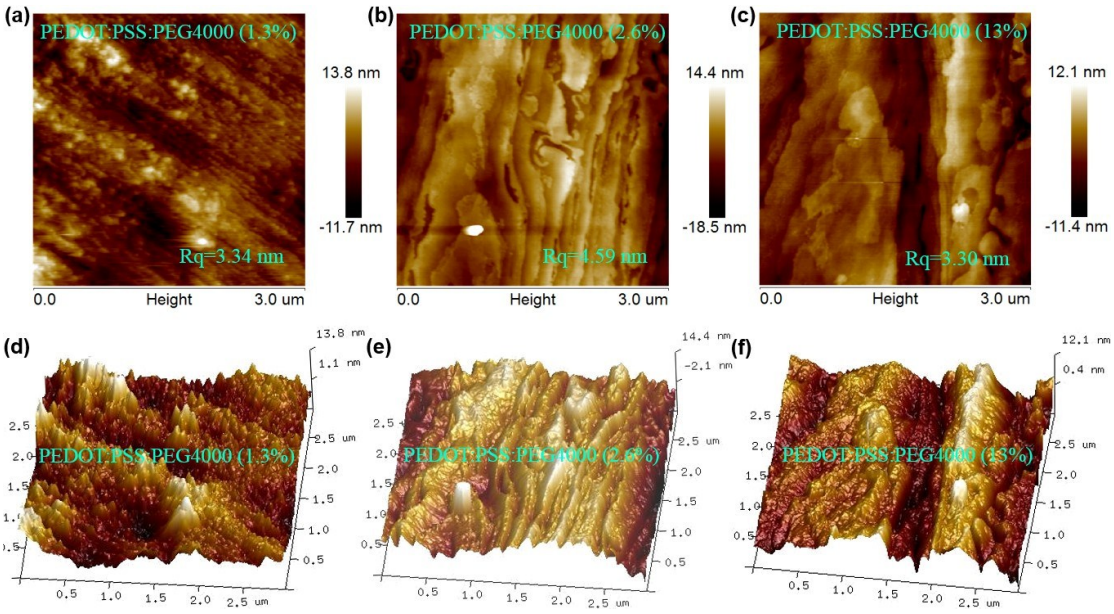

Figure S4. Atomic force microscope (AFM) height images of (a) PEDOT:PSS:PEG4000 (1.3%), (b) PEDOT:PSS:PEG4000 (2.6%), (c) PEDOT:PSS:PEG4000 (13%) and the corresponding three-dimensional images of (d) PEDOT:PSS:PEG4000 (1.3%), (e) PEDOT:PSS:PEG4000 (2.6%), (f) PEDOT:PSS:PEG4000 (13%), respectively.

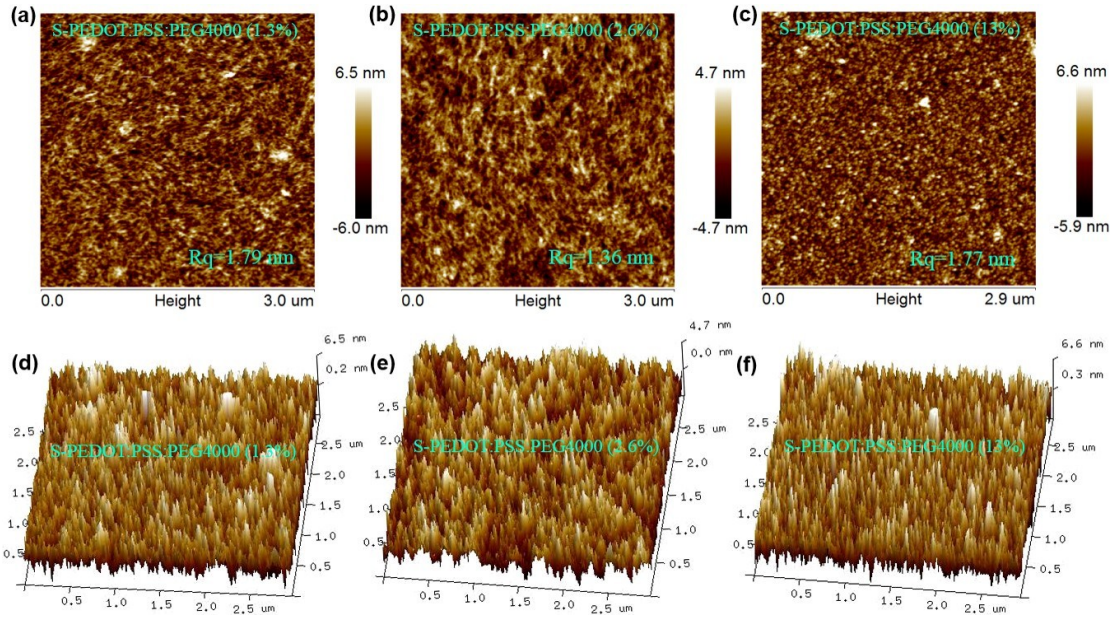

Figure S5. AFM height images of (a) S-PEDOT:PSS:PEG4000 (1.3%), (b) S-PEDOT:PSS:PEG4000 (2.6%), (c) S-PEDOT:PSS:PEG4000 (13%) and the corresponding three-dimensional images of (d) S-PEDOT:PSS:PEG4000 (1.3%), (e) S-PEDOT:PSS:PEG4000 (2.6%), (f) S-PEDOT:PSS:PEG4000 (13%), respectively.

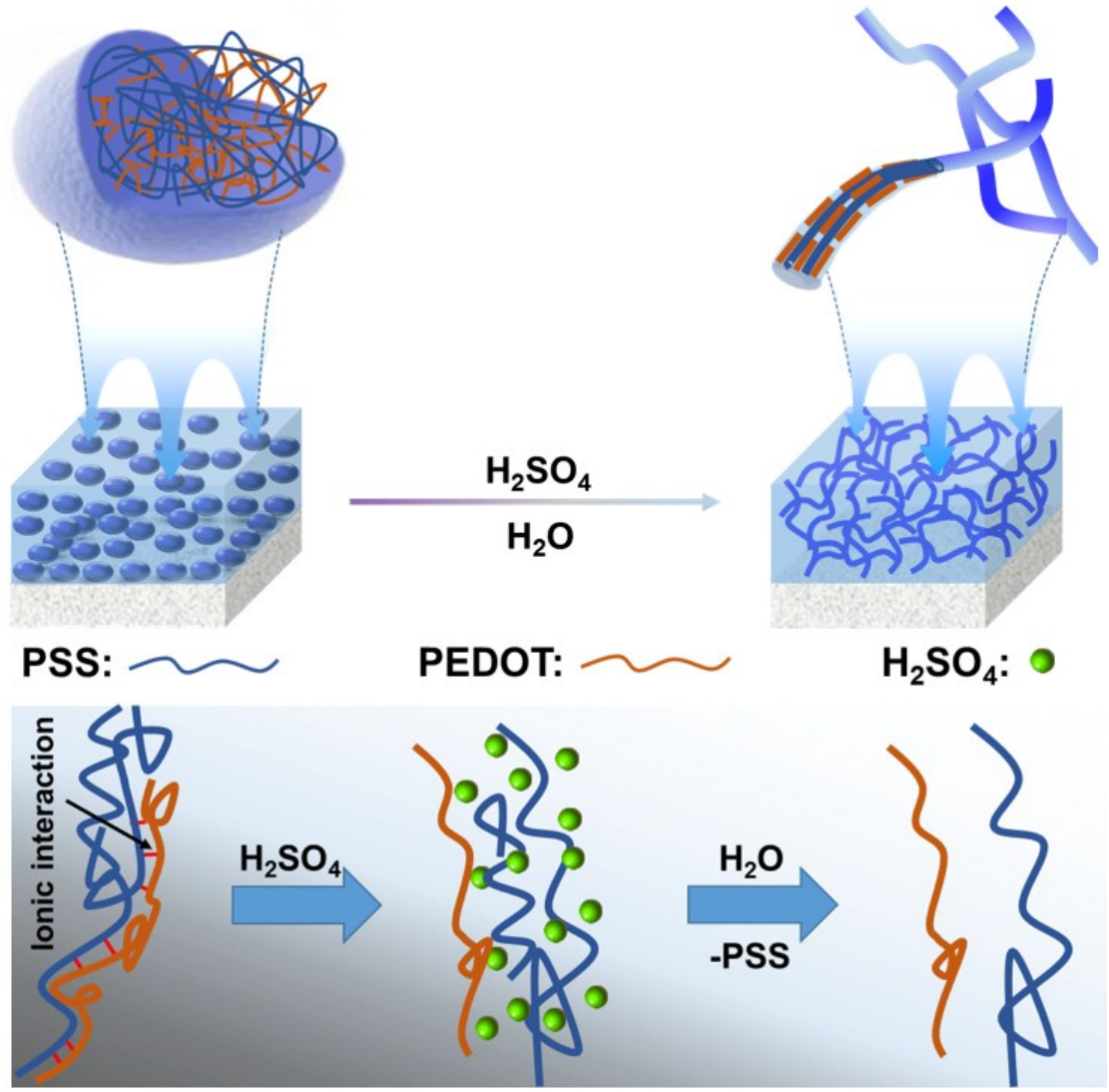

Figure S6. The schematic diagram of the configuration change of PEDOT:PSS during the treatment of H_2SO_4, as well as the simplified mechanism diagram.

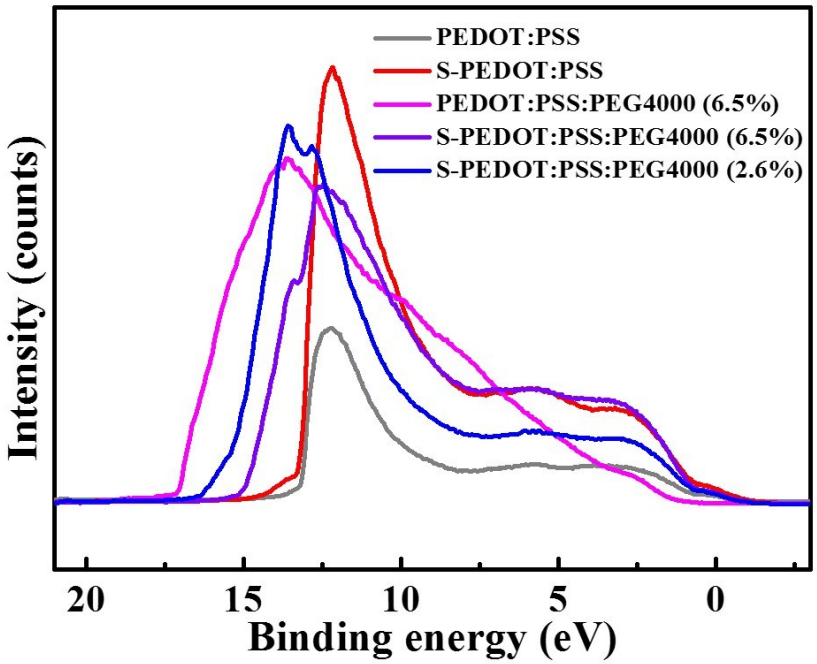

Figure S7. Ultraviolet photoelectron spectroscopy (UPS) spectra of PEDOT:PSS, S-PEDOT:PSS, PEDOT:PSS:PEG4000 (6.5%), S-PEDOT:PSS:PEG4000 (2.6%) and S-PEDOT:PSS:PEG4000 (6.5%).

Table S1. The work functions estimated via kelvin probe force microscope (KPFM) of gold (Au), PEDOT:PSS, S-PEDOT:PSS, PEDOT:PSS:PEG4000 (6.5%) and S-PEDOT:PSS:PEG4000 (6.5%), respectively.

Transparent electrode	Au	PEDOT:PSS	S-PEDOT:PSS	PEDOT:PSS: PEG4000 (6.5%)	S-PEDOT:PSS:PEG4000 (6.5%)
Work function (eV)	-5.1000	-4.8340	-4.7330	-4.1420	-4.5760

We select gold as the reference standard to estimate the work functions of the pristine and hybrid PEDOT:PSS films under the same conditions. The potential of the probe is -4.2650 eV.

Table S2. The work functions estimated by ultraviolet photoelectron spectroscopy (UPS) of PEDOT:PSS, S-PEDOT:PSS, PEDOT:PSS:PEG4000 (6.5%), S-PEDOT:PSS:PEG4000 (2.6%) and S-PEDOT:PSS:PEG4000 (6.5%), respectively.

Transparent electrode	PEDOT:PSS	S-PEDOT:PSS	PEDOT:PSS: PEG4000 (6.5%)	S-PEDOT:PSS:PEG4000 (2.6%)	S-PEDOT:PSS:PEG4000 (6.5%)
Work function (eV)	-5.5	-5.1	-3.6	-3.8	-3.7

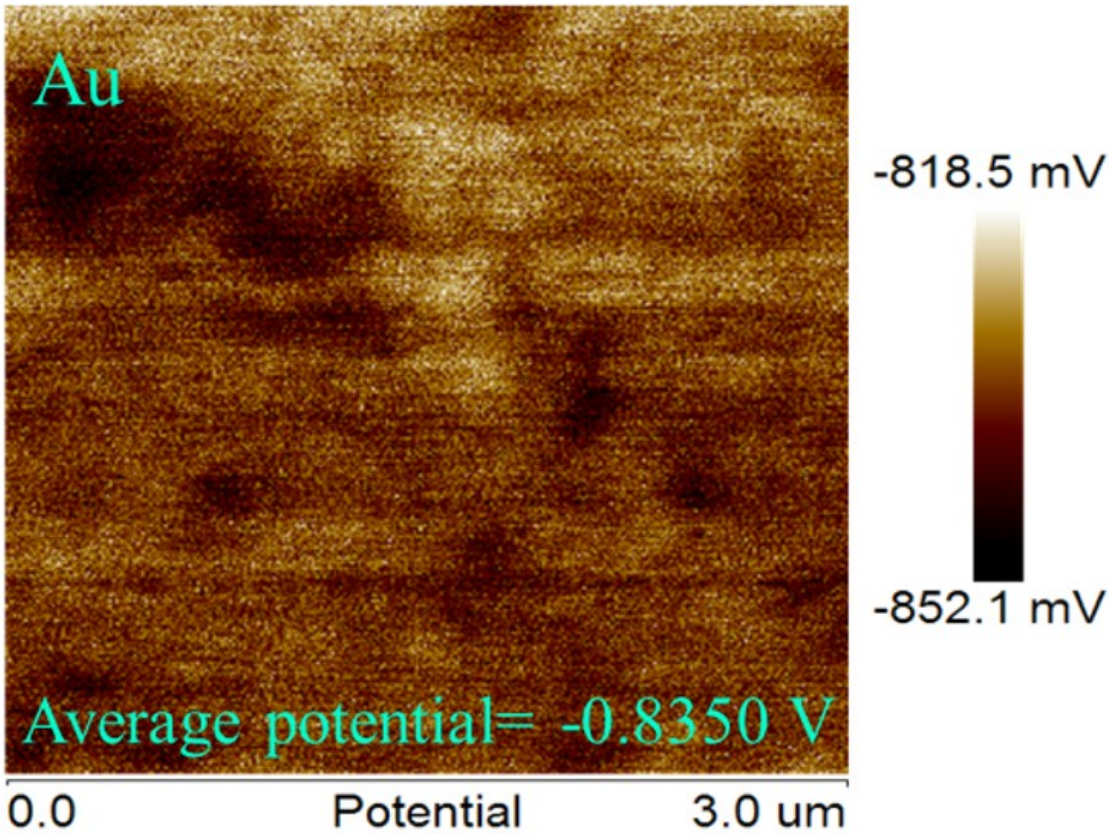

Figure S8. Kelvin probe force microscope (KPFM) image of gold (Au).

Table S3. Device parameters of the inverted structure based on glass substrate/cathode/zinc oxide (ZnO)/active layer/molybdenum trioxide (MoO_3)/silver (Ag).

Cathode	Active layer	J_{sc} (mA cm^{-2})	V_{oc} (V)	FF (%)	PCE (%)
PEDOT:PSS	P3HT:$PC_{61}BM$	2.788	0.592	45.7	0.8(1.0)[a]
S-PEDOT:PSS	P3HT:$PC_{61}BM$	8.318	0.558	43.4	2.0(2.3)[a]
S-PEDOT:PSS:PEG4000 (2.6%)	P3HT:$PC_{61}BM$	8.359	0.610	51.8	2.6(2.8)[a]
S-PEDOT:PSS:PEG4000 (6.5%)	P3HT:$PC_{61}BM$	9.003	0.620	57.0	3.2(3.3)[a]
S-PEDOT:PSS:PEG4000 (13%)	P3HT:$PC_{61}BM$	7.938	0.613	53.3	2.6(2.7)[a]
ITO	P3HT:$PC_{61}BM$	8.120	0.604	60.0	2.9(3.1)[a]
S-PEDOT:PSS	PTB7: $PC_{71}BM$	9.354	0.715	64.7	4.3(4.6)[a]
S-PEDOT:PSS:PEG4000 (6.5%)	PTB7: $PC_{71}BM$	15.880	0.744	68.6	8.1(8.3)[a]
ITO	PTB7: $PC_{71}BM$	13.045	0.726	66.5	6.3(6.5)[a]

a: The best PCE. Each cell had the effective area of 0.15 cm^2.

Table S4. Device parameters of the conventional structure based on glass substrate/anode/PEDOT:PSS Al 4083/active layer/lithium fluoride (LiF)/aluminum (Al).

Anode	Active layer	J_{sc} (mA cm^{-2})	V_{oc} (V)	FF (%)	PCE (%)
PEDOT:PSS	P3HT:$PC_{61}BM$	7.114	0.500	38.7	1.4(1.6)[a]
S-PEDOT:PSS	P3HT:$PC_{61}BM$	7.747	0.521	46.8	1.9(2.2)[a]
S-PEDOT:PSS:PEG4000 (2.6%)	P3HT:$PC_{61}BM$	8.255	0.537	48.6	2.2(2.6)[a]
S-PEDOT:PSS:PEG4000 (6.5%)	P3HT:$PC_{61}BM$	8.720	0.590	49.7	2.6(2.9)[a]
S-PEDOT:PSS:PEG4000 (13%)	P3HT:$PC_{61}BM$	7.300	0.584	48.5	2.1(2.3) [a]
ITO	P3HT:$PC_{61}BM$	8.353	0.610	60.5	3.1(3.5)[a]
S-PEDOT:PSS	PTB7: $PC_{71}BM$	12.745	0.732	67.3	6.3(6.6)[a]
S-PEDOT:PSS:PEG4000 (6.5%)	PTB7: $PC_{71}BM$	13.949	0.744	63.4	6.6(6.8)[a]
ITO	PTB7: $PC_{71}BM$	14.267	0.738	69.3	7.3(7.6)[a]

a: The best PCE. Each cell had the effective area of 0.15 cm^2.

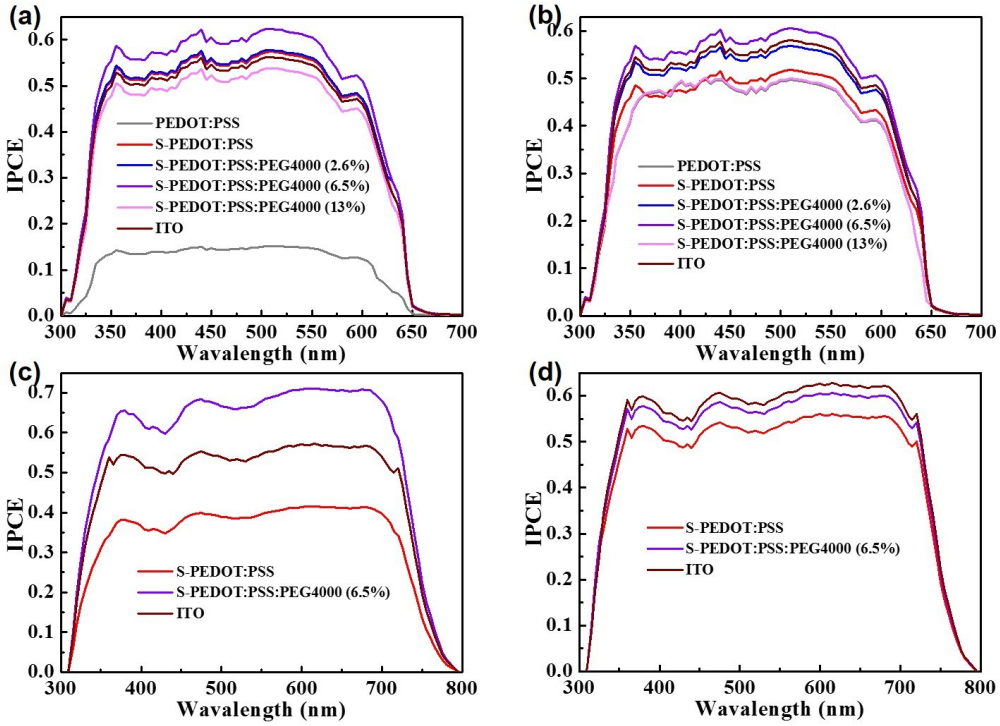

Figure S9. Incident photon to current conversion efficiency (IPCE) spectra of (a, c) based on the same inverted structure device with the active layer of P3HT:$PC_{61}BM$ and PTB7:$PC_{71}BM$, respectively. IPCE spectra of (b, d) depended on the same conventional structure device with the active layer of P3HT:$PC_{61}BM$ and P7B7:$PC_{71}BM$, respectively.